Phase transitions in surface segregation of Pt_cNi_{1-c} alloys from tight-binding Ising-model calculations

Bernard Legrand
Section de Recherches de Métallurgie Physique, Centre d'Etudes Nucleaires, 91191 Gif-sur-Yvette CEDEX, France

Guy Tréglia
Laboratoire de Physique des Solides, Bâtiment 510, Université Paris-Sud, 91405 Orsay CEDEX, France

François Ducastelle
Office National d'Etudes et de Recherches Aérospatiales, Boîte Postale 72, 92322 Châtillon CEDEX, France
(Received 15 May 1989; revised manuscript received 3 October 1989)

The tight-binding Ising model coupled with a mean-field approximation formulated as an area-preserving map is applied to surface segregation of Pt_cNi_{1-c} alloys. It allows us to reproduce the striking experimental data available for the low-index faces and in particular the face-related segregation reversal observed when going from the (111) to the (110) face. Moreover, it predicts some spectacular phase transitions of the concentration profiles as a function of temperature and bulk concentration.

I. INTRODUCTION

In the present paper the tight-binding Ising model[1,2] (TBIM) is used to describe from their electronic structure the energetics of atoms in surface-segregation phenomena for transition-metal alloys. Then, it is necessary to model the equilibrium state of the alloy by a given statistical approach. We use here the mean-field theory, which provides a useful first approximation. In this framework, surface segregation can be regarded as a one-dimensional problem in nonlinear dynamics with appropriate boundary conditions[3] and formulated as an area-preserving map (APM).[4] The corresponding phase portraits allow an easy and physical visualization of all possible solutions that can occur in a mean-field approximation—even in rather complex situations. These methods (TBIM-APM) are applied here to platinum-nickel alloys (Pt_cNi_{1-c}), which are exceptions to simple phenomenological criteria for surface segregation.[5] Actually, the segregation of Pt at any concentration of the disordered alloy observed in low-energy electron diffraction (LEED) experiments on the (111) surface[6] and its spectacular reversal[7] on the (110) face at $c=0.5$ (strong Ni segregation) can be explained neither by the difference in surface tension (quite negligible) nor by the elastic treatment[8] of the size effect, which always leads to the segregation of the solute. Initial progress[9] was made by the simultaneous use of an atomistic model and a relaxation process to minimize the strain energy calculated in a second-moment tight-binding framework.[10] As a result, the authors indeed found a surface sandwich with Pt on top whatever the concentration for the (111) and (100) faces,[9] in good agreement with experiments.[6,11] Moreover, contrary to the usual trends derived from phenomenological theories, they put in evidence a surprisingly smaller Pt enrichment for the (110) face. Unfortunately, the effect was not strong enough to lead to an Ni enrichment as in experiments.[7] A further improvement was to take into account a primary consequence of TBIM calculations, namely the enhancement at the surface of the effective pair interactions[1] (analogous to the mixing energy in phenomenological models[12]). This led the same authors to conclude an actual surface segregation reversal for the (110) face, i.e., a surface sandwich with Ni on top for $c>0.5$, the concentration profile remaining similar to that of the (111) face for $c<0.5$.[13] Although the former results are in good agreement with the corresponding experiments on $Pt_{0.5}Ni_{0.5}$, the latter appear to be conflicting with very recent experiments on $Pt_{0.1}Ni_{0.9}$ for which an Ni surface enrichment was found again.[14] A very similar study performed in the framework of the semiempirical embedded atom method (EAM) led to essentially the same conclusions as ours:[15] a surface sandwich with Pt on top whatever the concentration for the (111) and (100) faces and a sandwich with Ni(Pt) on top for $c>0.6$ ($c<0.3$). An interesting finding of the EAM study was a possible coexistence of both profiles for $0.3<c<0.6$ in Pt-Ni(110). Unfortunately, according to the author himself, a fundamental problem remained. The strongly oscillating concentration profile was not damped, even deep in the bulk. This illustrates the important and subtle problems related to the in-bulk termination of the concentration profile. We will show here that the use of phase portrait techniques provides an unambiguous way of solving this problem. In particular, it will allow us to reconcile experimental results and TBIM calculations and to solve the problem of the undamped oscillations in the EAM study. Moreover, it will bring to light the wide variety of concentration profiles and their possible modifications and phase transitions with temperature, bulk concentration, and crystallographic orientation.

The paper is organized as follows. In Sec. II we describe the TBIM formalism and in Sec. III the area-preserving mapping technique. We present in Sec. IV our

results for the surface segregation at the three low-index faces of Pt_cNi_{1-c} alloys and their evolution with temperature. Finally, in Sec. V, we discuss our results in relation to available experimental data and predict some spectacular phase transitions of the concentration profiles.

II. THE TIGHT-BINDING ISING MODEL (TBIM)

Let us summarize the main features of the TBIM.[1] From the electronic structure of the disordered alloy, one can derive an effective Ising Hamiltonian for segregation processes at surfaces of transition-metal alloys:

$$H^{\mathrm{TBIM}}=\sum_{n,i} p_n^i h_n^i+\tfrac{1}{2}\sum_{n,m,i,j}{}' p_n^i p_m^j V_{nm}^{ij}+\sum_{n,i} p_n^i H_n^{\mathrm{se},i} , \quad (1)$$

where p_n^i is the occupation number which is equal to 1 (0) if the site n is (not) occupied by an atom of type i and prime means $m\neq n$.

The first term in (1) is expressed in terms of the local field:

$$h_n^i=\frac{\mathrm{Im}}{\pi}\int^{E_F} dE \sum_{\lambda} \ln[1-(\varepsilon^i-\sigma_n)G_{nn}^{\lambda\lambda}(E)] . \quad (2)$$

The second term in (1) is written in terms of the *effective* pair interactions:

$$V_{nm}^{ij}=-\frac{\mathrm{Im}}{\pi}\int^{E_F} dE\ t_n^i(E)t_m^j(E)\sum_{\lambda,\mu} G_{nm}^{\lambda\mu}(E)G_{mn}^{\mu\lambda}(E) , \quad (3)$$

in which E_F is the Fermi level, ε^i the atomic d level for i atoms, and λ,μ the spin-orbital indices ($1\le\lambda,\mu\le 10$). $G_{nm}^{\lambda\mu}$ is the matrix element $\langle n,\lambda|G|m,\mu\rangle$ of the Green function in the disordered state, characterized by the self-energy σ_n described within the coherent-potential approximation (CPA);[16] t_n^i is the corresponding t matrix:

$$t_n^i(E)=\frac{\varepsilon^i-\sigma_n(E)}{1-[\varepsilon^i-\sigma_n(E)]\frac{1}{5}\sum_{\lambda} G_{nn}^{\lambda\lambda}(E)} . \quad (4)$$

It is worth noticing that this derivation indeed preserves local charge neutrality.[1] The third term accounts for a possible size effect: $H_n^{\mathrm{se},i}$ is calculated using simultaneously the atomistic tight-binding model and a relaxation process to minimize the strain energy of an atom i at site n.[9,10]

In the particular case of a binary alloy A_cB_{1-c} ($p_n^A=1-p_n^B=p_n$), Eq. (1) is written up to a constant:

$$H^{\mathrm{TBIM}}=\sum_n p_n\left[h_n-\sum_m{}' V_{nm}\right]+\sum_{n,m}{}' p_n p_m V_{nm}+\sum_n p_n H_n^{\mathrm{se}} , \quad (5)$$

with

$$h_n=h_n^A-h_n^B+\tfrac{1}{2}\sum_m{}'(V_{nm}^{AA}-V_{nm}^{BB}) ,$$

$$H_n^{\mathrm{se}}=H_n^{\mathrm{se},A}-H_n^{\mathrm{se},B} ,$$

and

$$V_{nm}=\tfrac{1}{2}(V_{nm}^{AA}+V_{nm}^{BB}-2V_{nm}^{AB}) . \quad (6)$$

In our surface problem, the relevant energetic quantities (as will be seen in Sec. III) are the differences between h_n, H_n^{se} for sites n belonging to a p plane parallel to the surface ($p=0$: surface, $p=1$: first underlayer . . .) and to the bulk:

$$\Delta h_p=h_{n\in p\text{ plane}}-h_{n\in\text{bulk}} , \quad (7)$$

$$\Delta H_p^{\mathrm{se}}=H_{n\in p\text{ plane}}^{\mathrm{se}}-H_{n\in\text{bulk}}^{\mathrm{se}} . \quad (8)$$

We give in Table I the values of ΔH_p^{se} in the dilute limits ($c\to 0$ or 1), from which ΔH_p^{se} is interpolated for intermediate concentrations.[9] Let us note that ΔH_p^{se} vanishes for $p\ge 2$.

By analogy with the phenomenological models,[5,12] Δh_p plays a role equivalent to the difference in p-layer tensions between pure constituents $\Delta\tau_p=\tau_p^A-\tau_p^B$, the p-layer tension τ_p^i being defined as the difference in energy between an atom in the p plane parallel to the surface and a bulk atom in the pure metal i. On the other hand, for a pair of bulk atoms, V_{nm} is strictly equivalent to the alloying energy Ω. The two major features of TBIM are that Δh_n is quasiconcentration independent and that the effective pair interaction V_{nm} is enhanced at the surface. More precisely, limiting the summation in (5) to first-neighbor interactions (which is justified from the electronic structure for fcc alloys[17]) and referring to the pair interactions V_{nm} as V if n *and* m are bulk atoms and as V_0 if n *or* m is at the surface, one finds

$$\begin{aligned} &V_0\cong 2\text{ V}\quad\text{for the (110) face ,}\\ &V_0\cong 1.5\text{ V}\quad\text{for the (111) and (100) faces .}\end{aligned} \quad (9)$$

This variation may be important as will be illustrated in the following for Pt_cNi_{1-c}. Let us point out, however, that Pt-Ni is a very peculiar system from the point of view of the general trends of order effects in transition-metal alloys. Actually the chemical disorder parameter ($\varepsilon^A-\varepsilon^B$) vanishes in that case and cannot explain the tendency of this alloy to exhibit ordered phases at low temperature. Then, it is necessary to put forward another type of disorder, related to the presence of spin-orbit coupling interactions on Pt atoms and not on Ni ones.[18] More precisely, the effective pair interactions due to spin-orbit effects present the same dependence with d band filling as those due to chemical disorder, but with the opposite sign, which leads to $V>0$ for Pt-Ni. Unfortunately, the calculated value is somewhat underestimated compared to the experimental value of order-disorder

TABLE I. Energy of the size mismatch effect for Pt-Ni in units of meV/at. for the three low-index surfaces. ΔH_p^i is the segregation energy due to the size effect on the p plane ($p=0$: surface, $p=1$: first underlayer) in the limits $c\to 0$ ($i=0$) and $c\to 1$ ($i=1$).

	ΔH_0^0	ΔH_0^1	ΔH_1^0	ΔH_1^1
(111)	−260	−40	0	+20
(100)	−280	+20	0	+30
(110)	−270	+90	−110	−20

temperature. Therefore, taking advantage of the previously mentioned analogy between Δh_p and $\Delta\tau_p$, and V and Ω, we will use here the experimental values of $\Delta\tau_0$ (Refs. 19 and 20) and Ω (or equivalently T_c) to determine Δh_0 and V: $\Delta h_0=\Delta h_1=\cdots=0$ eV, which is consistent with the almost equal surface tensions of Pt and Ni;[19,20] $V=84$ meV, which gives the correct critical temperature for the $L1_0$ ordered phase ($T_c\cong 900$ K) in exact thermodynamical calculations but a too large one ($T_c^*\cong 1970$ K) in the mean-field approximation ($T_c=0.45T_c^*$);[21] V_0/V is deduced from (9).

III. AREA-PRESERVING MAPPING (APM) IN THE MEAN-FIELD APPROXIMATION

The internal energy is obtained by averaging the Hamiltonian (5) over all configurations. The simplest (mean-field) approximation is to factorize the two-site correlation functions $\langle p_n p_m\rangle$ into the product of one-site correlation functions $\langle p_n\rangle\langle p_m\rangle$. Assuming that, in presence of a surface, the concentration can be different for planes parallel to this surface, one can define p-plane concentrations: $\forall n\in p$ plane $\langle p_n\rangle=c_p$. Averaging the entropy in the same way, we obtain the free energy:

$$F=\langle H\rangle+NkT\sum_p\left[c_p\ln c_p+(1-c_p)\ln(1-c_p)\right]-N\sum_p(c_p-c)\mu\ , \tag{10}$$

where N is the number of atoms per plane (constant in the absence of reconstruction) and μ is the chemical potential. The minimization of the free energy with respect to the layer concentration leads to the following system of coupled equations:

$$\forall p\ \frac{c_p}{1-c_p}=\frac{c}{1-c}\exp\left[-\left[\frac{\Delta H_p^{\rm seg}}{kT}\right]\right]\ , \tag{11}$$

where the segregation energy per plane $\Delta H_p^{\rm seg}$ is written

$$\begin{aligned}
\Delta H_0^{\rm seg}&=\Delta h_0+(Z+Z')(V-V_0)+Z'V+2[Z(V_0c_0-Vc)+Z'(V_0c_1-2Vc)]+\Delta H_0^{\rm se}\ ,\\
\Delta H_1^{\rm seg}&=\Delta h_1+Z'(V-V_0)+2[ZV(c_1-c)+Z'(V_0c_0+Vc_2-2Vc)]+\Delta H_1^{\rm se}\ ,\\
\Delta H_p^{\rm seg}&=2[ZV(c_p-c)+Z'V(c_{p-1}+c_{p+1}-2c)]\ ,
\end{aligned} \tag{12}$$

where Z and Z' are the numbers of first neighbors of a site in a given bulk layer parallel to the surface in the same plane and the first plane below (above), respectively. Let us point out here that these equations are valid when the coupling is between first-neighbor planes only. From the numerical point of view the nonlinear system [Eqs. (11) and (12)] can be rewritten

$$\begin{aligned}
c_1&=\frac{1}{2Z'V_0}\left[-kT\ln\frac{c_0}{1-c_0}-2ZV_0c_0+(Z+Z')V_0-\Delta h_0-\Delta H_0^{\rm se}+\mu\right]=f_1(c_0)\ ,\\
c_2&=\frac{1}{2Z'V}\left[-kT\ln\frac{c_1}{1-c_1}-2ZVc_1-2Z'V_0c_0+(Z+Z')V+Z'V_0-\Delta h_1-\Delta H_1^{\rm se}+\mu\right]=f_2(c_0,c_1)\ ,\\
c_{p+1}&=\frac{1}{2Z'V}\left[-kT\ln\frac{c_p}{1-c_p}-2ZVc_p-2Z'Vc_{p-1}+(Z+2Z')V+\mu\right]=f(c_{p-1},c_p)\ ,
\end{aligned} \tag{13}$$

where the chemical potential μ is determined by the bulk concentration in the disordered state c:

$$\mu=-(Z+2Z')V(1-2c)+kT\ln\frac{c}{1-c}\ . \tag{14}$$

It is worth noticing that most of the surface-segregation studies were performed by assuming that the concentration only varies at the surface ($c_0\neq c$, $c_1=c_2=\cdots=c$). This is obviously a too crude approximation which only becomes rigorous when $V=V_0=\Delta h_{p>0}=\Delta H_{p>0}^{\rm se}=0$. To go further, the usual procedure is to start from trial values of c_0, from which one can deduce c_1, then $c_2,\ldots,c_p$. The procedure is stopped when one reaches a p plane for which $|c_p-c|$ is small, up to an arbitrary accuracy. This method has been used in particular in the previous studies of Pt-Ni segregation.[2,9,13] Even though such a termination seems to be almost perfect for a drastic accuracy ($|c_p-c|<10^{-5}$), it suffers from a major drawback which can be seen in Fig. 1(a): if one allows the profile to go beyond this termination, instead of hitting exactly the bulk concentration, the iterations carry us far away. This is due to the inherent mathematical instability of the fixed point (c) of the iteration (to be distinguished from its physical stability).[22] To avoid this serious trouble, which can be put some big question marks even on the first part of the profile, we will use here an area-preserving mapping formulation of the mean-field theory.[4,22] The main idea is to remark that (13) can define the following two-dimensional mapping:

$$\begin{pmatrix}c_{p-1}\\ c_p\end{pmatrix}\xrightarrow{\mathcal{C}}\begin{pmatrix}c_p\\ c_{p+1}=f(c_{p-1},c_p)\end{pmatrix}\ . \tag{15}$$

In this framework, the bulk concentration is the only fixed point of the transformation $\mathcal{C}$ (at least, for $V>0$). The linearization of $\mathcal{C}$ around the fixed point (c) characterizes its topological nature. In the disordered state, the

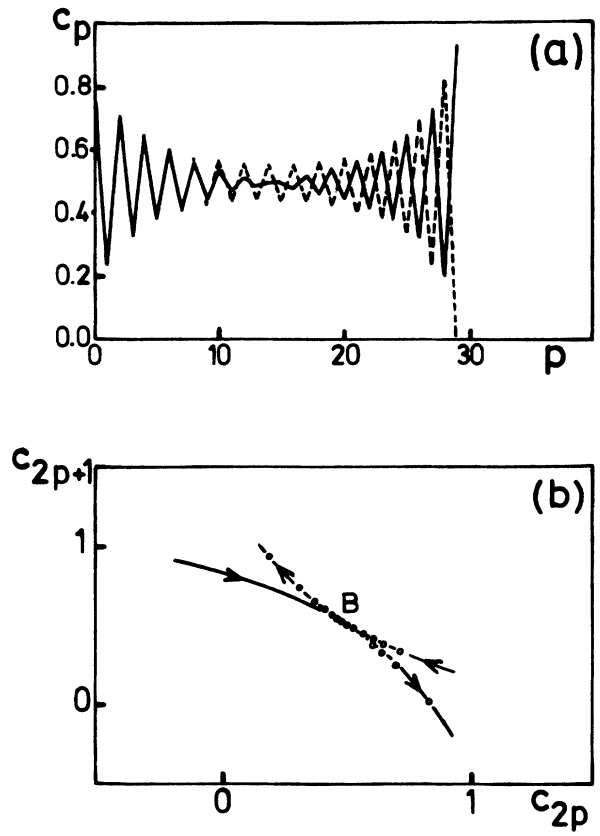

FIG. 1. (a) Concentration profiles of $Pt_{0.5}Ni_{0.5}(100)$ at $T=2000$ K obtained by the usual "trial and error" iteration method. (b) Phase portrait of $Pt_{0.5}Ni_{0.5}(100)$ at $T=2000$ K including the fixed point B, its inset and outset (— — —), and the open trajectories (●, ○) corresponding to the concentration profiles ——, ----, respectively, in (a).

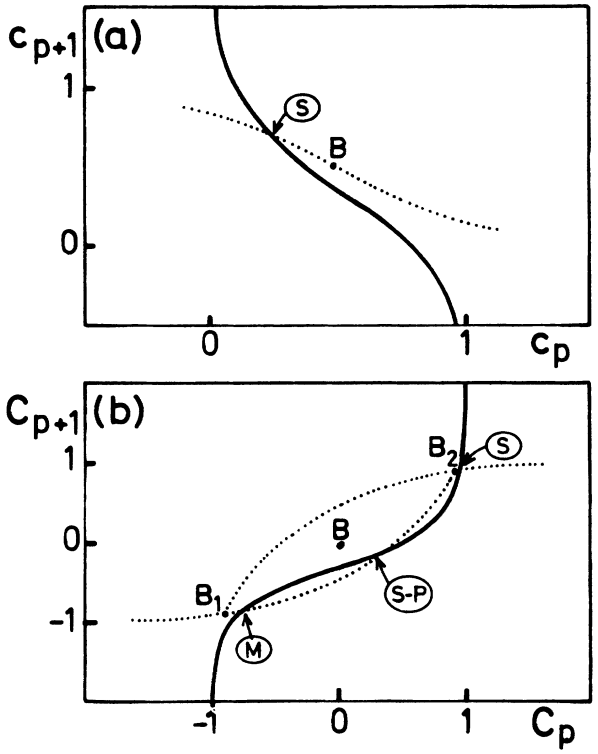

FIG. 2. Phase portraits of $Pt_{0.5}Ni_{0.5}(100)$ including the fixed point(s) $B_{(1,2)}$, their insets (· · · ·), and the boundary condition $c_2=g(c_1)$ (——) for $V_0/V=1.5$. (a) $T=2000$ K: (c_p,c_{p+1}) mapping. (b) $T=1200$ K: (C_p,C_{p+1}) mapping.

corresponding eigenvalues λ_1,λ_2 are real, negative, and such that $\lambda_1,\lambda_2\neq -1$ and $\lambda_1\lambda_2=1$. This is a so-called hyperbolic point with reflexion. The eigenvectors associated to λ_1 ($|\lambda_1|<1$) and λ_2 ($|\lambda_2|>1$) are the slopes of the insets (inflowing orbits) and outsets (outflowing orbits) of the fixed point, respectively. From a practical point of view, the outset is obtained after only a few iterations of $\mathcal{C}$ starting from any line passing through the fixed point (except its inset). On the other hand, the inset is drawn by iterations of $\mathcal{C}^{-1}$ (when the map is invertible) or equivalently as the symmetric of the outset under the transformation:

$$\begin{bmatrix} c_p \\ c_{p+1} \end{bmatrix} \rightarrow \begin{bmatrix} c_{p+1} \\ c_p \end{bmatrix} .$$

Such an inset is exhibited in Fig. 2(a) in the case of Pt_cNi_{1-c} (100) for $c=0.5$ and $T>T_c$. The reflexive character of the fixed point means that two successive iterations give points on both sides of it on its inset. This is related to the tendency of the alloy to order in the bulk, i.e., $V>0$: more precisely, a given plane interacting with its adjacent layers only, an enrichment on the former with respect to one species will be followed by a depletion on the latter.

The situation is more intricate when the bulk is ordered, below the critical temperature. Actually, if this ordered phase (characterized by the long range order parameter η) can be viewed as an alternate stacking of pure planes at $T=0$ [$c_{2p}=c(1+\eta)$; $c_{2p+1}=c(1-\eta)$ for $T_c>T>0$] along a given direction (for instance for $L1_0$ phase along [100] or [110] directions), and if the bulk is also described along this direction in (13)–(15), the fixed point $\binom{c}{c}$ becomes elliptic, i.e., numerically stable but physically unstable.[22] Actually, it is the fixed pair

$$\left\{ \begin{bmatrix} c(1+\eta) \\ c(1-\eta) \end{bmatrix}, \begin{bmatrix} c(1-\eta) \\ c(1+\eta) \end{bmatrix} \right\}$$

which is now physically stable. A well suited transformation to change this fixed pair into two fixed points is the following:

$$c_p \rightarrow C_p=(-1)^p(2c_p-1) .$$

Then the phase portrait of the (C_p,C_{p+1}) map presents one elliptic point $\binom{0}{0}$ and two simple (without reflection) hyperbolic ones $\binom{-\eta}{\eta},\binom{\eta}{\eta}$. The corresponding insets are shown in Fig. 2(b). Note that the two (thermodynamically stable) fixed points are joined by two heteroclinic trajectories, the inset of one point being the outset of the other one. Moreover, the central elliptic point $\binom{0}{0}$ has no inflowing or outflowing orbits. This phase portrait approach becomes of great use in the presence of a surface

since it identifies the solutions of the mean-field equation $c_{p+1}=f(c_{p-1},c_p)$ subject to the appropriate boundary conditions: $c_1=f_1(c_0)$ and $c_2=f_2(c_0,c_1)$ [see Eq. (13)]. In practice, the equilibrium concentration profile near the surface is obtained from the inflowing orbit which intersects the boundary condition $c_2=f_2(f_1^{-1}(c_1),c_1)=g(c_1)$ by keeping its part $(c_1,c_2,\ldots,c_p)$ between the intersection and the fixed point, then adding the surface concentration: $c_0=f_1^{-1}(c_1)$ (see Fig. 2). The main advantages of this technique are the following:

(i) It avoids the previously mentioned explosion which was due to the numerical impossibility to hit the fixed point exactly. Then, in the first part of the profile shown in Fig. 1(a), the open trajectory was getting near the fixed point along the inflowing orbits then went around it before running away in the second part along the outflowing orbits, which gives rise to the explosion [see Fig. 1(b)].

(ii) It allows an easy and physical visualization of the possible occurrence of multiple solutions [see Fig. 2(b)] in which case the one with the lowest value of the free energy functional should be chosen. A phase transition can occur when a variation of external parameters $(T,\ldots)$ lead to a switching of the minimum value of the free energy from one solution to another.

Let us now illustrate the potentialities of a simultaneous use of TBIM and APM first to interpret the puzzling experimental data concerning the surface segregation on the low-index faces of Pt-Ni alloys[6,7,11,14] and then to predict some spectacular phase transitions in concentration profiles with temperature.

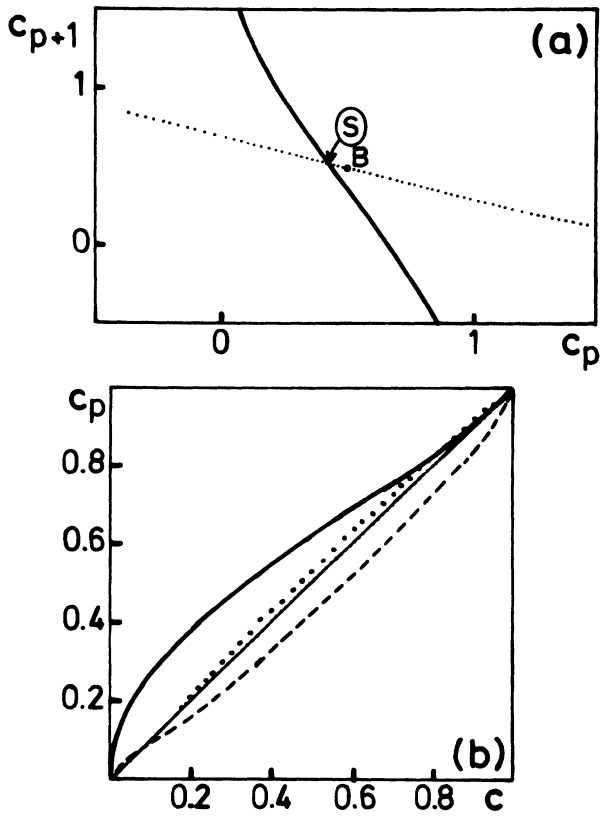

FIG. 3. (a) Phase portrait of $Pt_{0.5}Ni_{0.5}(111)$ at $T=1200$ K for $V_0/V=1.5$. The notations are the same as in Fig. 2(a). (b) Variation of c_0 (——), c_1 (— — —), and c_2 (· · · ·) as a function of c for $Pt_cNi_{1-c}(111)$ at $T=1200$ K for $V_0/V=1.5$.

IV. APPLICATION TO SURFACE SEGREGATION IN Pt-Ni ALLOYS

Let us briefly resume the experimental situation on the low-index faces of Pt_cNi_{1-c}. The first studied surface was the (111) one for which a surface sandwich with Pt on top was found on the whole concentration range.[6,11] Then a spectacular reversal of this concentration profile was observed on the (110) face, namely a surface sandwich with Ni on top, at least for $c=0.5$ (Ref. 7) and $c=0.1$.[14] In the latter case, a surprising bump[14] was exhibited in the curve c_0 versus c. Note that all these experiments were performed at about 1200 K, in the disordered state, well above the maximum critical temperature ($T_c\cong 900$ K at $c=0.5$). The following sections will give a physical insight on these striking phenomena.

A. Pt-Ni(111)

A previous theoretical study[9] in which (13) was solved by the usual "trial and error" method led to an oscillating profile with a Pt enriched surface, in agreement with experiments. This result, which is not strongly affected by a realistic variation of V at the surface,[2,13] is due to the competition between a predominant size effect and an ordering effect driven by the effective pair interaction V for $c<0.5$ and to the synergy between these effects for $c>0.5$.[9] Let us recall that the linear term Δh_p, which has been proven to be very close to the surface tension effect[1] (generally the leading term in surface-segregation processes), vanishes for Pt-Ni. One can wonder to what extent the explosive character of the concentration profile (Fig. 1), which was not observed in the previous works[2,9,13,15] due to the limited number of planes where the concentration was allowed to vary, could put some doubt on these results. In fact, they are fully confirmed by our TBIM-APM technique. Actually, at the experimental temperature ($T\cong 1200$ K) the phase portrait exhibits one solution only whatever the concentration [see Fig. 3(a) for $c=0.5$]. This remains true for any temperature. Let us emphasize that in our representation (c_p,c_{p+1}), the stacking of (111) planes does not "see" any of the ordered structures stabilized with first-neighbor interactions $(L1_0,L1_2)$.[17] In other words, the fixed point $\binom{c}{c}$ keeps its hyperbolic (with reflection) character up to $T=0$ K. A description of the ordered state, which is beyond the scope of this section, would require the introduction of intra-(111)-plane sublattices. The resulting $c_{p=0,1,2}$ versus c curves are shown in Fig. 3(b) for the values of Δh_p, V_0, V, and ΔH_p^{se} defined in Sec. II and Table I. They are very similar to our previous results[2,9,13] in spite of a different value of V (which was previously fitted to T_c within the mean-field approximation and then underestimated[21]) and to the EAM results.[15] The agreement with experiments[6] is qualitative, the oscil-

latory behavior being somewhat underestimated by the calculations.[2,9,13,15]

B. Pt-Ni(100)

From the electronic structure point of view, the (100) face appears very similar to the (111) one. The ratio V_0/V is equal to 1.5 and the size effect always favors the segregation of Pt, mainly for $c<0.5$. However, our mapping (C_p, C_{p+1}) allows us now to describe the $L1_0$ ordered phase at $c=0.5$. Thus, as explained in Sec. III, there is only one hyperbolic fixed point $\binom{0}{0}$ above T_c whereas three fixed points are presented below: $\binom{0}{0}$ which becomes elliptic (physically instable) and $\pm\binom{\eta}{\eta}$ which are hyperbolic [see Fig. 2(b)]. Let us recall that using an exact value of V and the mean-field approximation for a stacking along the [100] direction, one finds $T_c=1968$ K for $c=0.5$ and $T_c=708$ K for $c=0.1$ or 0.9. In the disordered state, one still finds one solution only over the whole range of temperature whereas in the ordered $L1_0$ phase, one sees in Fig. 2(b) that multiple solutions may occur. Two of them are true local minima S and M, the third one being a saddle point SP which then does not correspond to an equilibrium configuration. The concentration profiles corresponding to the unique minimum for $T>T_c$ and the two local minima for $T<T_c$ are shown in Fig. 4 for $c=0.1$, 0.5, and 0.9. Once more in the disordered state, they confirm our previous results: a strong Pt enrichment at the surface followed by an oscillatory concentration profile the more rapidly damped as T is high ($p=2$ for $c=0.1$ or 0.9 at $T=1200$ K) as can be seen from Figs. 4(b) and 4(c). Let us now comment on the behavior in the $L1_0$ ordered state analyzed along the variant built as an alternate stacking of pure planes. The corresponding concentration profiles are shown in Fig. 4(b) for the two local minima: S and M label, respectively, the stable and metastable solutions, their difference in free energy being of ~ 90 meV at $T=1200$ K. The stable solution corresponds to a termination of the bulk alternate stacking of planes with concentration $c(1\pm\eta)$ by a Pt-type surface plane, the metastable one being terminated by an Ni-type plane. We are faced here with a subtle semantic problem. In the usual surface-segregation terminology, the stable solution leads to a strong Pt enrichment of the surface ($c_0=0.89>c=0.5$) whereas in terms of ordered structure it can be considered as a slight depletion in Pt of the surface with respect to an ideal Pt-type bulk termination ($c_0=0.89<c_{2p}=0.95$). There exist no experimental data available in this ordered state, at least to our knowledge, but we can predict in view of the significant difference in free energy between the two solutions that only the stable one (S) should be observed. However, due to the presence of a quasipure Pt surface plane, the possibility of occurrence of a reconstruction analogous to the (5×20) one[23] in pure Pt cannot be ruled out. Its influence on the surface composition should require a simultaneous treatment of reconstruction and segregation which is currently in progress. To conclude with the (100) face, it is worth noticing that our results allow us to elucidate the "strange way in which the concentrations of layers far from the surface behave" in Lundberg's work.[15] Actually, the undamped oscillations he finds are due to his underestimation of T_c (calculated from an exact value of the heat of solution but within the mean-field approximation—see Sec. III and Ref. 21). Therefore his calculation at 1200 K is performed unintentionally in the ordered state.

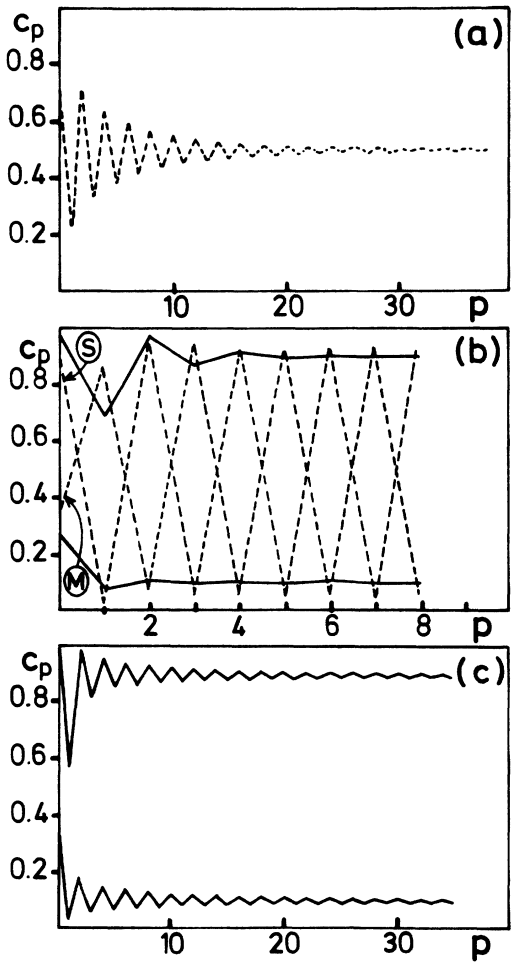

FIG. 4. Concentration profiles in $Pt_cNi_{1-c}(100)$ at three temperatures (a: 2000 K, b: 1200 K, c: 710 K) and three concentrations $c=0.1$ (——), 0.5 (— — —), 0.9 (——) for $V_0/V=1.5$.

C. Pt-Ni(110)

The (110) face presents, from the experimental point of view, the most intricate, and then the most interesting behavior. Moreover, from the theoretical point of view,[2,13,15] no study has been able up to now to account for the Ni enrichment observed both at $c=0.5$ (Ref. 7) and $c=0.1$.[14] From the electronic structure point of view, the (110) face strongly differs from the two previous close-packed faces. In particular the size effect—which indeed favors in this case the segregation of Pt for $c<0.7$ and on the contrary that of Ni for $c>0.7$ at the surface, associated with a segregation of Pt whatever the concentration in the first underlayer (see Table I)—competes with the ordering effect on the whole angle of concentra-

tion.[9] On the other hand, the ratio V_0/V is stronger ($\cong 2$) than for the other close-packed faces.[1] These two effects allowed us to predict a segregation reversal (surface sandwich with Ni on top) for $c > 0.5$ in the disordered state. Unfortunately, this calculation predicted a more usual behavior (i.e., surface sandwich with Pt on top) for $c < 0.5$, which was very recently invalidated by experiments performed at $T = 1200$ K and $c = 0.1$. It is worth noticing that the theoretical results obtained simultaneously on the same face by Lundberg within the EAM (Ref. 15) were very similar to ours and therefore cannot explain the experimental observations at $c = 0.1$. A remarkable result of the EAM study is the existence of two equilibrium profiles, a sandwich with Ni on top or at the opposite with Pt on top, with almost the same energies for $0.3 < c < 0.6$, the former solution being consistent with experiments and then called the stable one. Unfortunately this result, being obtained as for the (100) surface at 1200 K but in the ordered state (as shown by the similar undamped oscillations of concentration), cannot interpret experimental data collected at $T = 1200$ K but in the disordered state. It is then of prime importance to be able to perform the calculation both below and above T_c to check to what extent this multisolution character of surface segregation needs ordering in the bulk. The APM allows us to answer such a question, as previously illustrated for the (100) face. In the case of the (110) surface, one layer being coupled with the two below (above) adjacent planes, the mapping should become a four-dimensional one, then losing its appealing properties of easy visualization. In practice, this mapping can be approximated by a two-dimensional one by using effective interplane coordination numbers leading to the same critical temperature for $L1_0$ ordering, the electronic quantities of the TBIM ($\Delta h_p, \Delta H_p^{se}, V_0, V$) being calculated for the exact geometry. This gives for the (110) face $Z' = 3, Z'' = 0$ instead of $Z' = 4, Z'' = 1$ (Z'': number of first neighbors two planes above or below), when the $L1_0$ phase is analyzed along the variants built as alternate stackings of pure (110) planes. Thus, the critical temperatures are the same as for the (100) stacking: $T_c = 1968$ K (708 K) for $c = 0.5$ ($c = 0.1$ or $c = 0.9$). The corresponding phase portraits are exhibited in Fig. 5 above T_c for the three concentrations ($c = 0.1$, 0.5, and 0.9) and below for $c = 0.5$. Note that, for the sake of clarity, only the insets and the boundary conditions (for $V_0/V = 1$ and $V_0/V = 2$) are represented. Moreover, to make easier the comparison between ordered and disordered bulk state, we show a (C_p, C_{p+1}) mapping whatever the temperature at $c = 0.5$ whereas a (c_p, c_{p+1}) mapping is used for $c = 0.1$ and 0.9. The most striking feature is that the enhancement of the effective pair interaction involving one surface site at least, derived from TBIM ($V_0 = 2V$), is essential to stabilize a second concentration profile above

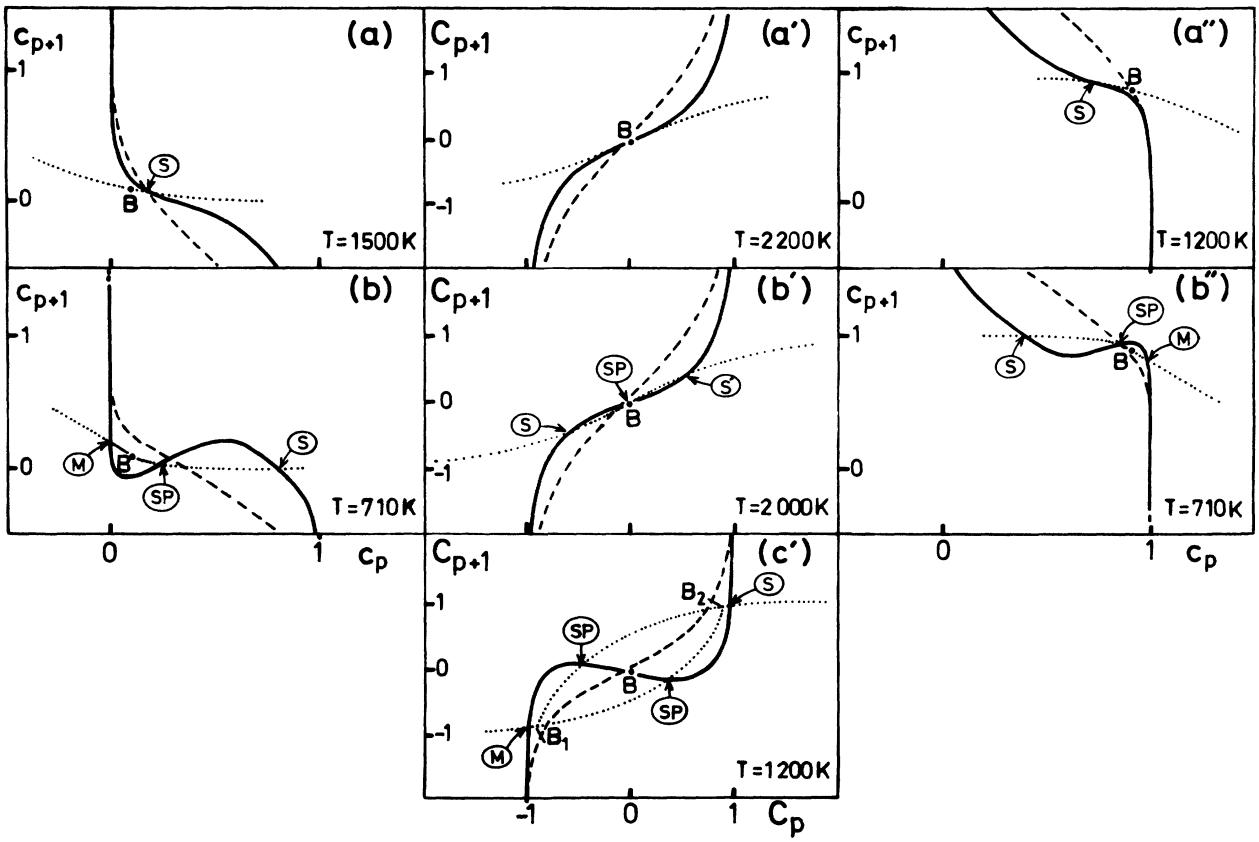

FIG. 5. Phase portraits of $Pt_cNi_{1-c}(110)$ for three concentrations $c = 0.1$ (a,b), 0.5 (a',b',c'), and 0.9 (a",b"), as a function of temperature. Only the insets (· · · ·) of the fixed point $B_{(1,2)}$ are shown with the boundary condition $c_2 = g(c_1)$ for $V_0/V = 2$ (——) and $V_0/V = 1$ (— — —). The (c_p, c_{p+1}) mapping is used for $c = 0.1$ and $c = 0.9$ and the (C_p, C_{p+1}) one for $c = 0.5$.

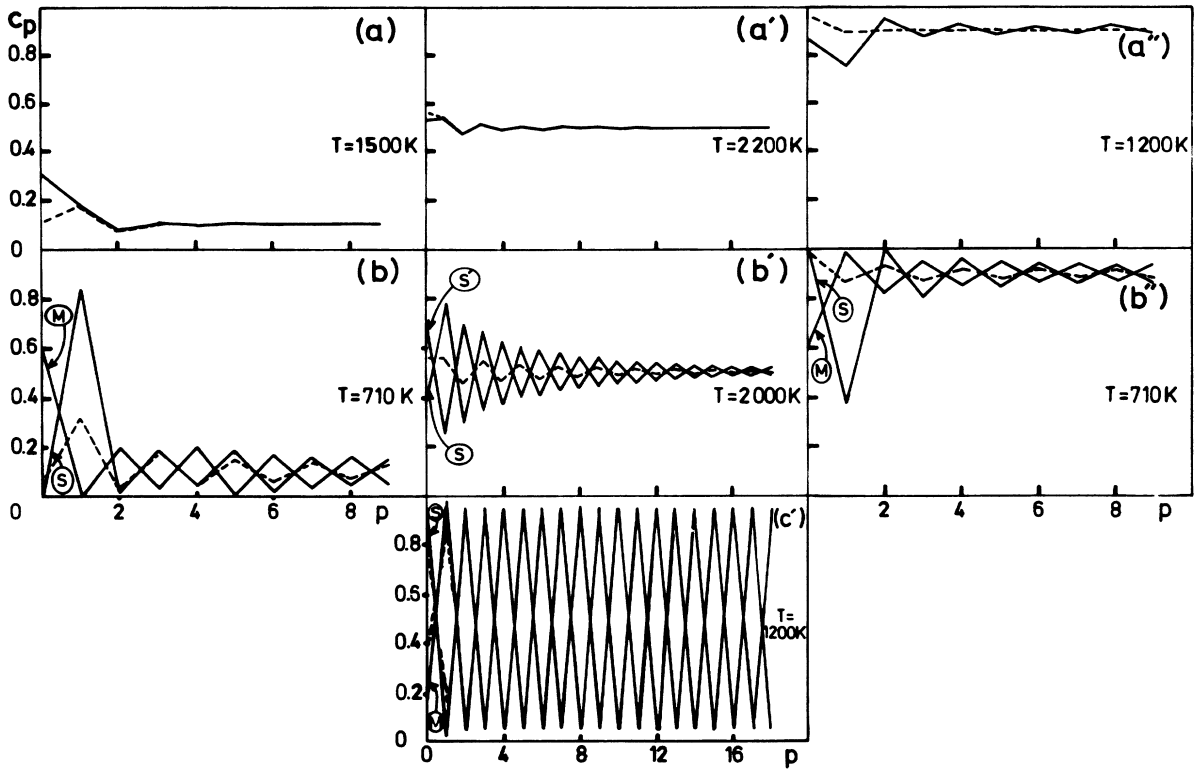

FIG. 6. Concentration profiles for Pt-Ni(110) corresponding to the phase portraits of Fig. 5, using $V_0/V=2$ (——) and $V_0/V=1$ (— — —).

T_c [Figs. 5(b), 5(b'), and 5(b'')]. More precisely, in a given range of temperature above T_c, the boundary condition for $V_0/V=2$ intersects the insets three times (instead of only once for $V_0/V=1$) leading to two local minima and one saddle point (SP). The minimum free-energy criterion determines which of the minima is the stable one (S) or the metastable one (M). As a function of increasing temperature, the true minimum free energy may switch from one point to the other leading to phase transition before M vanishes at higher temperature [Figs. 5(a), 5(a'), and 5(a'')]. In the ordered $L1_0$ phase [Fig. 5(c')] two minima exist also for $V_0/V=1$, which means that even usual phenomenological theories can predict such bistabilities. The two additional intersections occurring for $V_0/V=2$ are nothing but saddle points. A more physical insight on the problem requires the knowledge of the concentration profiles corresponding to these minima. They are given in Fig. 6 for the same temperatures and concentrations. Let us discuss for each concentration the evolution of the concentration profile with temperature.

1. $c=0.5$

At sufficiently high temperature one recovers our previous results[9,13] whatever V_0/V, i.e., a slight Pt enrichment on the first two layers followed by the usual rapidly damped oscillations [Fig. 6(a')], mainly due to the size effects on these two planes.[9] Decreasing the temperature up to the critical temperature, the behavior for $V_0/V=2$ becomes drastically different from that for $V_0/V=1$ which evolves only slightly. Actually, in this range of temperature (2175 K$\rightarrow$1968 K), two different concentration profiles (S and S' in phase opposition), quasi-indiscernible from the energetics point of view ($F_S-F_{S'}\cong -2.10^{-4}$ eV), appear for $V_0/V=2$, namely two sandwiches with Ni(S) or Pt(S') on top, respectively, presenting slowly damped oscillations up to ~ 10 layers, the former being the most stable. Finally, below T_c, the two types of profiles (S,M) coexist (now even for $V_0/V=1$) but the oscillation is undamped since the bulk is ordered. Once more, we are faced with the terminological problem previously mentioned in Sec. IV B. These profiles exhibit surface enrichments $c_0=0.94$ (0.16) with respect to the disordered bulk concentration but surface depletions compared to their counterparts in the ordered bulk: $c_{2p}=0.95$ (0.05). This confirms that the EAM calculation[15] performed at $T=1200$ K unintentionally in the bulk ordered state is improperly used to describe surface segregation in the bulk disordered state. Concerning the free energies, the two possible concentration profiles can be strongly distinguished: $F_S-F_M\cong -10^{-3}$ eV but now S corresponds to the sandwich with Pt on top. To summarize, our main result at $c=0.5$ is the coexistence at $T>T_c$ of the two concentration profiles: sandwich with Pt on top and with Ni on top. Let us recall that only one solution is found for $T>T_c$ when $V_0/V=1$.

2. $c=0.1$

The most striking features are essentially the same as for $c=0.5$, namely the appearance for $V_0/V=2$ of two equilibrium profiles in phase opposition in a wide range of temperature (710–1200 K) above T_c (708 K), contrary to the only one observed profile for $V_0/V=1$, as can be seen in Fig. 6(b) for instance. More precisely, between 710 and 1140 K the stable equilibrium profile (S) is the sandwich with Ni on top and a very strong Pt enrichment in the first underlayer. Then between 1140 and 1250 K, the minimum switches to the sandwich with Pt on top which becomes the unique solution at higher temperature [see Fig. 6(a) for $T=1500$ K]. In this latter case, the concentration profile on the first three layers becomes monotonous which is an unusual behavior for alloys such as $V>0$ (ordering tendency) and is only possible due to the enhancement of V at the surface.

3. $c=0.9$

Once more two oscillating solutions in phase opposition coexist in a narrower range of temperature above T_c, for $V_0/V=2$. Contrary to the previous cases, they significantly differ in free energy in this whole range of temperature. As a consequence the stable solution remains always the same, evolving continuously to the unique solution at higher temperature. The corresponding concentration profile is characterized by a strong Pt depletion in the first underlayer, the surface concentration varying only slightly around the bulk concentration ($0.85 \le c_0 \le 1.00$ when $1200\ \text{K} \ge T \ge 710$ K).

V. PHASE TRANSITIONS OF THE CONCENTRATION PROFILES

Let us now develop the main consequence of the variation with temperature of the concentration profiles mentioned in Sec. IV C. Complementary information can be derived from Fig. 7 in which the surface concentration (c_0) is plotted as a function of the bulk concentration at two temperatures. These curves deserve some comments. At high temperature (1900 K) we observe the following sequence of surface enrichments as a function of the bulk concentration:

(i) $0<c<0.35$: The solution is unique with Pt enrichment.

(ii) $0.35<c<0.5$: There is bistability of two solutions, the previous solution becoming metastable and the most stable one being the new one which is Ni enriched. As a consequence, there is a jump of surface concentration at $c=0.35$.

(iii) $0.5<c<1$: There is a new jump at 0.5 towards the first solution (Pt enriched), the Ni-enriched one becoming metastable up to $c=0.6$ where it vanishes. Then one observes a continuous crossover of the now unique solution which is Pt enriched up to $c=0.7$ and Ni enriched for $0.7<c<1$.

These essential features are unchanged at lower temperature, only the limits of the previous domains being changed. These variations of the concentration limits lead to phase transitions with temperature which are illustrated in Fig. 8. More precisely, considering (c_0-c) as an order parameter, we predict a first order transition at about 1140 K for $c=0.1$ which should not be observed in usual phenomenological theories in which $V_0=V$. The situation is more complex for $c=0.5$. Decreasing the temperature we first have a unique solution (Pt enrichment) which switches to an Ni-enriched one after a second order phase transition at 2175 K, the free energies of both profiles remaining comparable ($|\Delta F|<2.10^{-4}$ eV) in a wide range of temperature (2175 K$\rightarrow$1968 K). Let us emphasize that this surface phase transition occurs significantly above the bulk order-disorder transition. Then, at the critical bulk temperature ($T_c=1968$ K) a

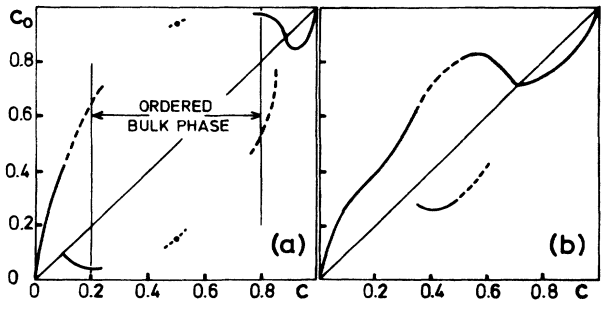

FIG. 7. Variation of c_0 as a function of c for $Pt_cNi_{1-c}(110)$ at $T=1200$ K (a) and $T=1900$ K (b) for $V_0/V=2$. The stable solution is labeled (——) and the metastable one (— — —). Note that in (a), only the points corresponding to $c=0.5$ have been calculated in the ordered region.

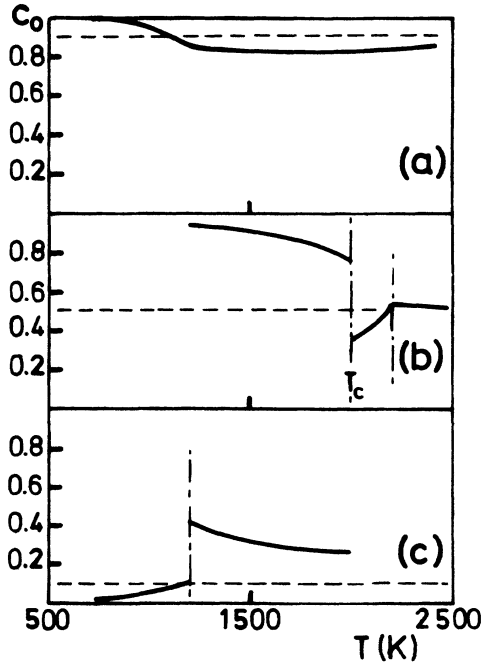

FIG. 8. Variation of c_0 considered as a surface order parameter as a function of temperature in $Pt_cNi_{1-c}(110)$ for three concentrations: $c=0.9$ (a), 0.5 (b), and 0.1 (c).

strongly first order surface phase transition occurs, leading to a surface enriched with Pt at lower temperature. Let us recall that these phenomena are due to the enhancement of V at the surface. Finally, the variation of c_0 versus T at $c=0.9$ presents a third kind of behavior. Actually, no first order transition is expected but only a crossover within the same solution from a Ni-enriched solution ($T>1150$ K) to the Pt-enriched one ($T<1150$ K). A funny consequence of this behavior is an increase of the Ni enrichment with increasing temperature in the range 1150–2000 K, which is not to be related to the vibrational entropy arguments used by some authors to explain the apparent increase of Pt surface concentration with temperature at Pt-Rh alloy surfaces.[24]

To conclude this section, let us compare our results to the very detailed LEED experimental data available on Pt-Ni surfaces. Let us first recall that we reproduce (semiquantitatively) the surface sandwich with Pt on top observed at $T=1200$ K in the whole range of concentration for the (111) surface.[6] Moreover, we do not predict any phase transition with temperature on this face, at least in the disordered bulk state. These conclusions remain valid for the (100) face. However, the problem of a possible reconstruction is set up and experiments on this face should be of interest. From the experimental point of view, the (110) face presented a spectacular face-related segregation reversal at about 1200 K for $c=0.5$ (Ref. 7) and $c=0.1$,[14] leading to a sandwich with Ni on top. This is indeed what we find in the disordered state. However, for $c=0.5$ we must keep in mind the necessary scaling in temperature due to the mean-field approximation, which prevents us from a direct quantitative comparison with experiments at $T=1200$ K. This scaling would require us to use instead our results at $T=1900$ K [see Fig. 7(b)], which obviously decreases the Ni enrichment of the surface, and therefore the amplitude of the oscillation. When our calculations can be directly compared with experiments, i.e., for $c=0.1$ at $T\cong 1120$ K, one finds $c_0=0.11$, $c_1=0.48$, and $c_2=0.02$ in almost perfect agreement with the corresponding LEED data:[14] $c_0=0.06\pm 0.04$, $c_1=0.52\pm 0.02$, and $c_2=0.10\pm 0.10$. Moreover, the c_0 versus c curve shown in Fig. 7(a) exhibits an unusual bump at $c\cong 0.1$, which has indeed been observed in LEED experiments.[14] It can be useful to point out the origin of the difference between our present results and our previous ones[2,13] concluding in a Pt enrichment for $c<0.5$. This was due to our iterative procedure which converged always to one of the possible multiple solutions, and not necessarily to the most stable one. This is obviously a major advantage of the present APM technique to avoid this drawback.

VI. PHYSICAL ORIGIN OF THE SURFACE-SEGREGATION REVERSALS

In view of the complexity of concentration profile behaviors illustrated in Fig. 8, one can wonder about their physical origin, i.e., on the respective roles of the different factors involved in the segregation energies $\Delta H_0^{\rm seg}, \Delta H_1^{\rm seg}\ldots$ [Eq. (12)]. Let us first point out that the peculiarity of the Pt-Ni system originates from the vanishing of the surface local field Δh_0 [Eqs. (6) and (7)]. Actually, when Δh_0 is not negligible, it is generally the most important term and leads to the segregation of the most tension-active element. In the present case, the segregation energy reduces to the combination of the size mismatch term $\Delta H_p^{\rm se}$ and the ordering term $\Delta H_p^{\rm ord}$:

$$\Delta H_p^{\rm seg}=\Delta H_p^{\rm ord}+\Delta H_p^{\rm se}\ , \tag{16}$$

with

$$\begin{aligned}
\Delta H_0^{\rm ord}&=2V_0[Z(c_0-c)+Z'(c_1-c)]+\Delta H_0^{\rm asymp}\ ,\\
\Delta H_1^{\rm ord}&=2[V_0Z'(c_0-c)+VZ(c_1-c)+VZ'(c_2-c)]+\Delta H_1^{\rm asymp}\ ,\\
\Delta H_p^{\rm ord}&=2[VZ'(c_{p-1}-c)+VZ(c_p-c)+VZ'(c_{p+1}-c)]+\Delta H_p^{\rm asymp}\ ,
\end{aligned} \tag{17}$$

and

$$\begin{aligned}
\Delta H_0^{\rm asymp}&=(1-2c)[(Z+Z')(V-V_0)+Z'V]\ ,\\
\Delta H_1^{\rm asymp}&=(1-2c)Z'(V-V_0)\ ,\\
\Delta H_{p\geq 2}^{\rm asymp}&=0\ .
\end{aligned} \tag{18}$$

The competition between $\Delta H_p^{\rm ord}$ and $\Delta H_p^{\rm se}$ is at the origin of the variety of behaviors as a function of the surface orientation, the bulk concentration, and the temperature.

Let us first mention that the size mismatch energy $\Delta H_p^{\rm se}$ calculated within the atomistic tight-binding model detailed in Refs. 9 and 10 is bulk concentration dependent as in the elastic treatment.[8] However, contrary to the elasticity result,[8] this dependence is strongly asymmetric. Due to the anharmonic properties of the interatomic interactions, the impurity segregates at the surface, the more as it is the biggest. Moreover, $\Delta H_0^{\rm se}$ is now orientation dependent. In particular, the asymmetry of the c dependence of $\Delta H_0^{\rm se}$ decreases from the close-packed to the open surfaces, due to larger surface relaxations in the latter case (see Table I).

The role of the ordering term $\Delta H_p^{\rm ord}$ is more complex due to its dependence with local concentrations c_{p-1}, c_p, c_{p+1}. This is illustrated in Eq. (17) in which we have separated the part of $\Delta H_p^{\rm ord}$ which depends on $\delta c_p=(c_p-c), \delta c_{p-1}, \delta c_{p+1}$ from the asymptotic part (18) corresponding to the limit $T\to\infty$ ($\delta c_p=0, \forall_p$). However, some general trends can be put forward in the framework of the usual phenomenological approaches[12] in which $V_0/V=1$. In that case, for $V>0$, $\Delta H_0^{\rm ord}$ favors segregation of the majority element in the absence of other factors ($\Delta H_0^{\rm se}=\Delta h_0=0$); in the presence of another factor (here $\Delta H_0^{\rm se}\neq 0$), $\Delta H_0^{\rm ord}$ tends to reduce the segre-

gation due to this factor; the ordering effect leads to an oscillating concentration profile, at least if $\Delta H_1^{se}=\Delta h_1=0$, as usual in empirical models.

Unfortunately, electronic structure calculations[1] have shown that $V_0/V\neq 1$, which could invalidate the above assertions. This can be seen on the asymptotic values (18) which change sign when V_0/V increases. In particular, some critical values of this ratio can be derived from the vanishing of ΔH_0^{asymp}:

$$\left[\frac{V_0}{V}\right]_c=\frac{Z+2Z'}{Z+Z'}\ , \tag{19}$$

which leads to $(V_0/V)_c=1.33$ and 1.5 for the (111) and (100) faces and 1.7 for our approximate (110) face. The TBIM derived values (9) are somewhat larger (1.5, 1.5, and 2, respectively) indicating that the sign of ΔH_0^{asymp} in the present work is opposite to that obtained in the empirical approaches.

In fact, it is clear that the ordering effect cannot be isolated in the same way as the size effect; ΔH_p^{ord} is determined by the equilibrium concentration profile and then indirectly depends on the size effect $\Delta H_0^{se}, \Delta H_1^{se}$. It is then important to keep in mind this coupling when analyzing the variations with temperature of ΔH_p^{se} and ΔH_p^{ord} $(p=0,1)$ which are illustrated in Figs. 9 and 10 for the (111) and (110) orientations, respectively.

Let us first discuss the case of the (111) face of Pt_cNi_{1-c}. One sees in Fig. 9 that, whatever the concentration, the size effect $(\Delta H_0^{se}<0)$ always favors surface segregation of Pt (the big atom) especially in the dilute limit $(c\to 0)$, its contribution being almost negligible on the first underlayer $(\Delta H_1^{se}\cong 0)$. In the almost whole range of temperature, the ordering effect at the surface (ΔH_0^{ord}) plays against the size effect as in phenomenological theories. In the asymptotic regime of high temperature, δc_0, $\delta c_1\to 0$ so that the ordering effect [which reduces to its asymptotic value (18)] is indeed decoupled from the size effect. In this case, $\Delta H_0^{ord}=\Delta H_0^{asymp}$ favors segregation of the minority species, contrary to phenomenological theories. Let us recall that this is due to the TBIM value of $V_0/V=1.5$ $[>(V_0/V)_c=1.33]$. On the first underlayer, the ordering effect ΔH_1^{ord} for T sufficiently low tends to impose an oscillating profile by reacting to surface segregation. In the higher temperature regime, the asymptotic part of ΔH_1^{ord} becomes

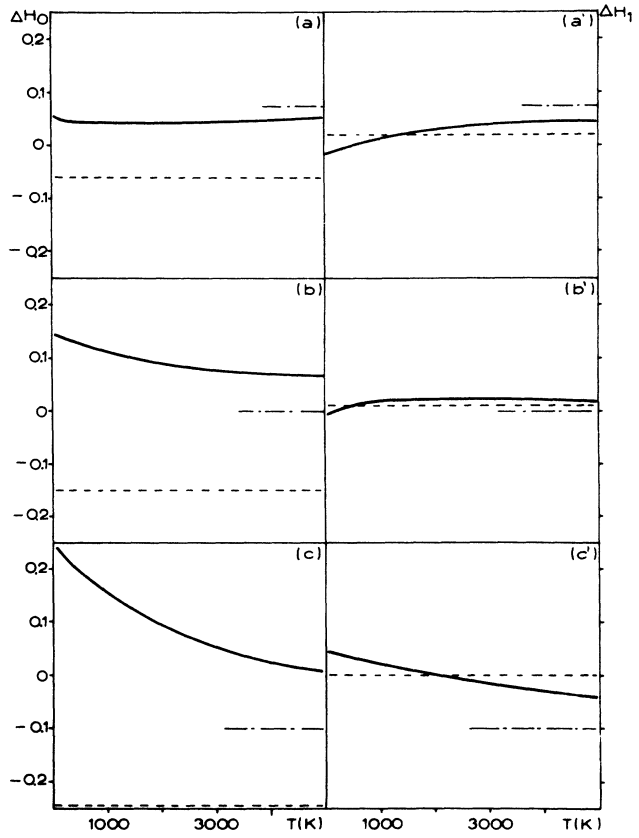

FIG. 9. Variation of ΔH_p^{se} (Ref. 9) and ΔH_p^{ord} [Eq. (17)] ($p=0$: surface, $p=1$: first underlayer) as a function of temperature for $Pt_cNi_{1-c}(111)$ and $c=0.8$ (a: $p=0$; a': $p=1$), $c=0.5$ (b: $p=0$; b': $p=1$), and $c=0.1$ (c: $p=0$; c': $p=1$). Solid line: ΔH_p^{ord}; dot-dashed line: ΔH_p^{asymp} [see Eq. (18)]; dashed line: ΔH_p^{se}.

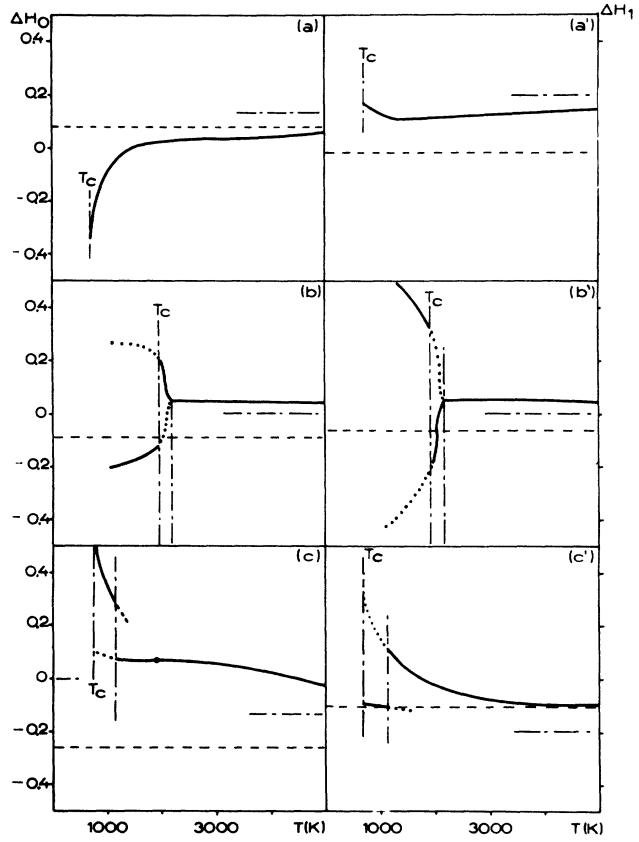

FIG. 10. Variation of ΔH_p^{se} (Ref. 9) and ΔH_p^{ord} [Eq. (17)] ($p=0$: surface, $p=1$: first underlayer) as a function of temperature for $Pt_cNi_{1-c}(110)$ and $c=0.9$ (a: $p=0$; a': $p=1$), $c=0.5$ (b: $p=0$, b': $p=1$), and $c=0.1$ (c: $p=0$; c': $p=1$). Solid line: ΔH_p^{ord} stable solution; dotted line: ΔH_p^{ord} metastable solution; dot-dashed line: ΔH_p^{asymp} [see Eq. (18)]; dashed line: ΔH_p^{se}.

preponderant. Remarking that $\Delta H_1^{\text{asymp}} = \Delta H_0^{\text{asymp}}$ for the TBIM values of V_0/V, one then recovers on the first underlayer a tendency to segregation of the minority element. This can lead even to a monotonous profile (c_0, c_1) as in the case $c = 0.1$, $T > 2000$ K, which is completely unusual in ordering alloys.[12]

Let us now analyze the puzzling behavior of c_0 with T exhibited in Fig. 8. To this end, we report in Fig. 10 the corresponding variation of ΔH_p^{ord} and ΔH_p^{se}. First, one recovers a change of sign of the size effect ΔH_0^{se} with bulk concentration (at $c \cong 0.6$) as in elasticity but with a very different physical origin. Actually, due to the important surface relaxation (contraction of the first interlayer distance[10]) of the (110) face, the surface plane is a zone in compression which favors segregation of the small atom (Ni) when the minority element. For the same reason, due to the oscillatory character of the relaxation profile, the first underlayer is a zone in dilatation which attracts the big atoms leading to a segregation of Pt whatever c. This illustrates how it is essential to properly account for surface relaxation effects in surface-segregation studies.

As for the (111) face, the ordering term ΔH_0^{ord} plays against the size effect in the disordered state in a range of temperature sufficiently far from the asymptotic regime and in the latter case favors segregation of the minority element. Similarly, ΔH_1^{ord} forces the profile to be oscillating up to the asymptotic regime in which one recovers the tendency to segregation of the minority element $(\Delta H_1^{\text{asymp}} = 1.5 \Delta H_0^{\text{asymp}})$. On the contrary, below T_c for $c = 0.5$ there is a synergy between ordering and size effects, which is quite natural when the ordered structure can be described as an alternate stacking of pure planes parallel to the surface. Indeed, in that case, two terminations coexist when only the ordering effect is present: pure surface with respect to one element or the other. When another effect (here size effect) is added, the termination which insures the synergy between both effects is favored. Finally, the first order character of the surface phase transition at T_c for $c = 0.5$ and the existence of a surface phase transition in the disordered state for $c = 0.1$ is only due to the enhancement of V at the surface $(V_0/V = 2)$ as previously illustrated by Fig. 6.

VII. CONCLUSION

Since our TBIM-APM calculation gives a correct description of all the existing and amazing experimental results concerning surface segregation in Pt-Ni alloys, we have reasons to believe that our predictions are sufficiently well grounded and spectacular to deserve new experiments on Pt-Ni (110) as a function both of temperature and concentration. In particular, the Ni enrichment should switch to a Pt enrichment by studying the (110) face, either for $c = 0.05$ at $T = 1200$ K, or at $c = 0.10$ at $T \geq 1500$ K. Moreover, the behavior for alloys rich in Pt $(c > 0.6)$ should exhibit a crossover from an Ni enrichment $(c \to 1)$ to a Pt enrichment (for instance $c = 0.9$ at $T = 1200$ K). Finally, experiments in the ordered bulk phase should be of great interest to illustrate the competition between surface and bulk phase transitions and the relation between the surface structure of ordered alloys and surface segregation in disordered alloys. Let us add one last remark. Going beyond the mean-field approximation could induce some changes in the precise values of the above derived critical temperatures and concentrations and in the predicted order of the phase transitions. Thus Monte Carlo simulations are currently in progress.

ACKNOWLEDGMENTS

We are indebted to P. Maugain and A. Finel for many enlightening discussions and to G. Martin for his constant interest during this work.

[1] G. Tréglia, B. Legrand, and F. Ducastelle, Europhys. Lett. **7**, 575 (1988).

[2] B. Legrand, G. Tréglia, and F. Ducastelle, in *Atomistic Simulation of Materials*, edited by V. Vitek and D. J. Srolovitz (Plenum, New York, 1989), p. 461.

[3] V. I. Arnold and A. Avez, *Ergodic Problems of Classical Mechanics* (Benjamin, New York, 1968).

[4] R. Pandit and M. Wortis, Phys. Rev. B **25**, 3226 (1982).

[5] A. R. Miedema, Z. Metallkd. **69**, 455 (1978); F. F. Abraham and C. R. Brundle, J. Vac. Sci. Technol. **18**, 506 (1981); J. R. Chelikowsky, Surf. Sci. Lett. **139**, L197 (1984).

[6] Y. Gauthier, Y. Joly, R. Baudoing, and J. Rundgren, Phys. Rev. B **31**, 6216 (1985); R. Baudoing, Y. Gauthier, M. Lundberg, and J. Rundgren, J. Phys. C **19**, 2825 (1986).

[7] Y. Gauthier, R. Baudoing, M. Lundberg, and J. Rundgren, Phys. Rev. B **35**, 7867 (1987).

[8] D. McLean, *Grain Boundaries in Metals* (Oxford University, London, 1957); J. Friedel, Adv. Phys. **3**, 446 (1954).

[9] G. Tréglia and B. Legrand, Phys. Rev. B **35**, 4338 (1987).

[10] F. Ducastelle, J. Phys. (Paris) **31**, 1055 (1970); D. Tomanek, A. A. Aligia, and C. A. Balseiro, Phys. Rev. B **32**, 5051 (1985); V. Rosato, M. Guillopé, and B. Legrand, Philos. Mag. **59**, 321 (1989).

[11] J. C. Bertolini, J. Massardier, P. Dedicher, B. Tardy, B. Imelik, Y. Jugnet, Tran Minh Duc, L. de Temmerman, C. Creemers, H. Van Hove, and A. Neyens, Surf. Sci. **119**, 95 (1982); L. de Temmerman, C. Creemers, H. Van Hove, A. Neyens, J. C. Bertolini, and J. Massardier, Surf. Sci. **178**, 888 (1986).

[12] F. L. Williams and D. Nason, Surf. Sci. **45**, 377 (1974).

[13] B. Legrand and G. Tréglia, in *The Structure of Surfaces II*, edited by J. F. Van der Veen and M. A. Van Hove (Springer-Verlag, Berlin, 1987), p. 167.

[14] Y. Gauthier, R. Baudoing, and J. Jupille, Phys. Rev. B **40**, 1500 (1989).

[15] M. Lundberg, Phys. Rev. B **36**, 4692 (1987).

[16] B. Velicky, S. Kirkpatrick, and H. Ehrenreich, Phys. Rev. **175**, 747 (1968).

[17] A. Bieber, F. Gautier, G. Tréglia, and F. Ducastelle, Solid State Commun. **39**, 149 (1981).

[18] G. Tréglia and F. Ducastelle, J. Phys. F **17**, 1935 (1987).

[19] W. R. Tyson and W. A. Miller, Surf. Sci. **62**, 267 (1977); Y. K. Kumikov and K. B. Khokonov, J. Appl. Phys. **54**, 1346 (1983); C. G. Walker and D. C. Peacock, Appl. Surf. Sci. **35**,

173 (1988–89).
[20]S. M. Foiles, M. I. Baskes, and M. S. Daw, Phys. Rev. B **33**, 7983 (1986).
[21]D. de Fontaine, Solid State Phys. **34**, 73 (1979).
[22]M. H. Jensen and P. Bak, Phys. Rev. B **27**, 6853 (1983).
[23]P. Heilmann, K. Heinz, and K. Müller, Surf. Sci. **83**, 487 (1979).
[24]F. C. M. J. M. Van Delft and B. E. Nieuwenhuys, Surf. Sci. **162**, 538 (1985); F. C. M. J. M. Van Delft, A. D. Van Langeveld, and B. E. Nieuwenhuys, *ibid.* **189/190**, 1129 (1987).